THE JOURNAL OF BIOLOGICAL CHEMISTRY VOL. 291, NO. 25, pp. 13028–13039, June 17, 2016


# Wnt Protein Signaling Reduces Nuclear Acetyl-CoA Levels to Suppress Gene Expression during Osteoblast Differentiation*

Received for publication, December 9, 2015, and in revised form, April 1, 2016 Published, JBC Papers in Press, April 20, 2016, DOI 10.1074/jbc.M115.708578

**Courtney M. Karner**[‡1], **Emel Esen**[‡§], **Jiakun Chen**[§], **Fong-Fu Hsu**[¶], **John Turk**[¶], **and Fanxin Long**[‡§¶‖2]

*From the* [‡]*Department of Orthopaedic Surgery,* [§]*Division of Biology and Biomedical Sciences,* [‖]*Department of Developmental Biology, and* [¶]*Department of Medicine, Washington University School of Medicine, Saint Louis, Missouri 63131*

**Developmental signals in metazoans play critical roles in inducing cell differentiation from multipotent progenitors. The existing paradigm posits that the signals operate directly through their downstream transcription factors to activate expression of cell type-specific genes, which are the hallmark of cell identity. We have investigated the mechanism through which Wnt signaling induces osteoblast differentiation in an osteoblast-adipocyte bipotent progenitor cell line. Unexpectedly, Wnt3a acutely suppresses the expression of a large number of genes while inducing osteoblast differentiation. The suppressed genes include *Pparg* and *Cebpa*, which encode adipocyte-specifying transcription factors and suppression of which is sufficient to induce osteoblast differentiation. The large scale gene suppression induced by Wnt3a corresponds to a global decrease in histone acetylation, an epigenetic modification that is associated with gene activation. Mechanistically, Wnt3a does not alter histone acetyltransferase or deacetylase activities but, rather, decreases the level of acetyl-CoA in the nucleus. The Wnt-induced decrease in histone acetylation is independent of β-catenin signaling but, rather, correlates with suppression of glucose metabolism in the tricarboxylic acid cycle. Functionally, preventing histone deacetylation by increasing nucleocytoplasmic acetyl-CoA levels impairs Wnt3a-induced osteoblast differentiation. Thus, Wnt signaling induces osteoblast differentiation in part through histone deacetylation and epigenetic suppression of an alternative cell fate.**

A major challenge in modern biology is to understand the mechanism of cellular differentiation in metazoans. Although sharing the same genes, the diverse cell types of a given organism each exhibit a unique profile of gene expression. Gene expression in turn is regulated by the local chromatin milieu at each gene locus. At the molecular level, this milieu reflects epigenetic modifications of both DNA (*e.g.* methylation) and the associated proteins such as histones (1). Among histone modifications, acetylation and methylation have been most extensively studied. Whereas histone acetylation is often associated with active gene expression, the roles of histone methylation are more complex depending on the position of the lysine residue being modified (2, 3). Thus, epigenetic modifications of the chromatin are at the core of cell differentiation. Although it is known that a small number of developmental signals are chiefly responsible for cell differentiation, it is not well understood how these signals confer the epigenetic modifications necessary for cell type-specific gene expression. Studies to date have focused mostly on the direct downstream transcription factors that engage specific genomic loci and recruit chromatin-modifying enzymes. However, it is becoming increasingly clear that various metabolic intermediates, such as $NAD^+$, acetyl-CoA, and α-ketoglutarate, can also influence the epigenetic modifications of the chromatin milieu (4–6). Whether or not developmental signals may exert epigenetic regulation through intermediate metabolites has not been explored.

Wnt signaling is a critical regulator of cell differentiation in metazoans both during embryogenesis and in postnatal tissue homeostasis (1, 2. Wnt proteins are secreted glycoproteins that activate multiple intracellular signaling cascades. In the most well characterized pathway, Wnt stabilizes β-catenin, which enters the nucleus and interacts with the Lef/Tcf family of transcription factors to activate downstream target genes. In addition, Wnt proteins can also activate the Rho family of small GTPases, the $Ca^{2+}$ pathway, PKCδ, mTORC1, and mTORC2 (7–13). Through the various effectors, Wnt signaling has been recently shown to regulate cellular metabolism in both normal and cancerous cells (14–17). Wnt signaling has been shown to regulate chromatin modifications through β-catenin, which forms complexes with a number of chromatin-modifying enzymes including histone acetyltransferases (HAT),[3] TIP60, and CBP/p300, the H3K4 histone methyltransferase MLL1·MLL2 complex, and the H3K79 histone methyltransferase Dot1-containing complex (18–21). However, potential epigenetic regulation by Wnt through β-catenin-independent mechanisms is largely unexplored.

Wnt signaling has emerged as an important mechanism regulating bone formation in mammals (22). In the mouse embryo, deletion of β-catenin or both Lrp5 and Lrp6 in the skeletogenic progenitors abolishes osteoblast differentiation, indicating that Wnt signaling through β-catenin is critical for embryonic osteoblastogenesis (23–27). In postnatal life, loss- and gain-of-function mutations in LRP5 cause low and high bone mass syn-

* This work was supported by National Institutes of Health Grants AR060456 (to F. L.), 5F32AR060674 (to C. M. K.), P41-RR00954 (to J. T.), P60-DK20579 (to J. T.), and P30-DK56341 (to J. T.). The authors declare that they have no conflicts of interest with the contents of this article. The content is solely the responsibility of the authors and does not necessarily represent the official views of the National Institutes of Health.

[1] Present address: Dept. of Orthopaedic Surgery, Duke University School of Medicine, Durham, NC 27710.

[2] To whom correspondence should be addressed. E-mail: flong@wustl.edu.

[3] The abbreviations used are: HAT, histone acetyltransferase; TCA, tricarboxylic acid; L, L-cell; CM, conditioned media; HDAC, histone deacetylase; qPCR, quantitative PCR; dn-, dominant negative; TSA, trichostatin A; Acly, ATP citrate lyase; Pdk1, pyruvate dehydrogenase kinase 1.

dromes, respectively, in humans (28–30). Moreover, deficiency in SOST, a secreted inhibitor that prevents the binding of WNT to LRP5 or LRP6, results in high bone mass in human patients (31, 32). In the mouse, deletion of Lrp5 causes osteopenia (33, 34), whereas loss of SOST increases bone mass (35). The mechanism through which Wnt signaling stimulates osteoblast differentiation, however, remains incompletely understood.

Here we present evidence that Wnt signaling induces osteoblast differentiation in part through rapid epigenetic suppression of genes responsible for alternative cell fates. Specifically, Wnt3a acutely reduces nuclear acetyl-CoA, the necessary substrate for histone acetyltransferases, resulting in a global decrease in histone acetylation. These data reveal a novel mechanism by which Wnt signaling suppresses alternative cell fates through modulation of acetyl-CoA levels in the cell.

## Experimental Procedures

*Cell Culture*—ST2 cells were cultured in α-MEM (Gibco) supplemented with 10% FBS (Invitrogen), 5 mM glucose, and 2 mM glutamine. All experiments were carried out at a seeding density of 13,000 cells/cm$^2$. Wnt treatments were initiated 24 h after plating by replacing the medium with α-MEM supplemented with 50 ng/ml recombinant Wnt3a (R&D Systems) *versus* vehicle control (0.1% CHAPS in PBS) or by replacing the medium with α-MEM diluted 1:1 with Wnt3a- or L-cell (L)-conditioned medium (CM). In the Dkk1 experiment the cells were pretreated with 500 ng/ml Dkk1 for 1 h before treatment with Wnt3a and Dkk1 for 6 h. BMP2 treatments were initiated by replacing the medium with α-MEM supplemented with either 300 ng/ml recombinant BMP2 (R&D Systems) or vehicle control (0.1% HCl). In indicated experiments growth media was supplemented with 10 ng/ml trichostatin A or 20 mM sodium acetate. For Wnt3a- or BMP2-induced mineralization, cells were treated with Wnt3a or BMP2 with or without the other reagents as indicated for 72 h and then switched to mineralization medium (α-MEM supplemented with 50 mg/ml ascorbic acid (Sigma) and 10 mM β-glycerophosphate (Sigma)) for 6 days with a change of medium every 48 h. Mineralization was assayed by von Kossa staining.

*Overexpression of Dominant Negative TCF4 (dnTCF4), Wnt7b, Wnt10b, or Pyruvate Dehydrogenase Kinase 1 (Pdk1)*—ST2 cells were infected with retroviral vectors expressing either empty vector or dnTCF4, Wnt7b, or Wnt10b for 12 h followed by a 12-h recovery. The viruses were constructed as previously described (23). For overexpression of Pdk1, ST2 cells were co-infected with lentiviruses expressing FUW-rtTA and FUW-tetO-myc-Pdk1-IRES-GFP or the control FUW-tetO-IRES-GFP and then induced with 100 ng/ml doxycycline. Pdk1 protein expression was detected by Western blotting with a specific antibody (Enzo #ADI-KAP-PK112, 1:1000 dilution).

*shRNA or siRNA Knockdowns*—Lentiviral vectors expressing shRNA against β-catenin and Pparg were obtained from the RNAi core at Washington University School of Medicine. The lentiviral vector pLKOpuro was modified to express shRNAs targeting β-catenin, Pparg, or either LacZ or RFP as negative controls (Table 1). The shRNA-expressing lentiviral vector was co-transfected with plasmids pMD2.g and psPax2 into 293 cells. Viral containing media were collected and filtered. ST2 cells were plated at 13,000 cells/cm$^2$ and infected for 12 h and then recovered for 36 h in regular media. ATP citrate lyase (Acly) was knocked down with the siRNA On-Targetplus SMART pool (Dharmacon) as follows. ST2 cells were plated at 4200 cells/cm$^2$ and transfected with 25 nM SMARTpool #104112 and 0.25 μl of DUO transfection reagent (Dharmacon) for 48 h.

**TABLE 1**
**shRNA sequences used in this study**

| Gene symbol | Insert sequence |
|---|---|
| *LacZ* | GCGATCGTAATCACCCGAGTG |
| *RFP* | ACAACAGCCACAACGTCTATA |
| *β-catenin*-A9 | GCGTTATCAAACCCTAGCCTT |
| *β-catenin*-A7 | CCATCACAGATGTTGAAACAT |
| *Pparg*-1 | GCCTCCCTGATGAATAAAGAT |
| *Pparg*-2 | CCTGGTTTCATTAACCTTGAT |

*Histone Deacetylase (HDAC) and HAT Activity Assays*—HDAC activity was measured in 50 μg of nuclear extract with the Fluor-de-lys HDAC fluorometric activity assay kit (Enzo Life Sciences, BML-AK500). HAT activity was measured in 50 μg of nuclear lysate by a colorimetric HAT assay (Abcam, ab65352). Each assay was performed in technical triplicate from three independent experiments.

*RNA Isolation and qPCR*—Total RNA was isolated from cultured cells using the RNAeasy kit with on-column DNase treatment (Qiagen). Reverse transcription was performed using 100 ng of total RNA with the iScript cDNA synthesis kit (Bio-Rad). Reactions were set up in technical and biological triplicates in a 96-well format on an ABI StepOne Plus using SYBR green chemistry (SsoAdvanced, Bio-Rad). The PCR conditions were 95 °C for 3 min followed by 40 cycles of 95 °C for 10s and 60 °C for 30s. Gene expression was normalized to 18S rRNA, and relative expression was calculated using the $2^{-(\Delta\Delta Ct)}$ method. Primers were used at 0.1 μM, and their sequences are listed in Table 2. PCR efficiency was optimized, and melting curve analyses of products were performed to ensure reaction specificity.

*RNA-Seq*—Poly-A RNA was isolated from 20 μg of total RNA using Oligo-dT beads. mRNA was fragmented and reverse-transcribed into double-stranded cDNA. cDNA was blunt-ended followed by the addition of A base to 3′ end and the ligation of sequencing adapters to the ends. The fragments then underwent PCR amplification for 12 cycles. The resulting libraries were sequenced using the Illumina HiSeq-2000 as single reads extending 42 bases (GTAC, Washington University). The raw data were demultiplexed and aligned to the reference genome (mm9) using TopHat. Both Cufflinks and Partek Genomic Suite were used independently to assemble transcripts and analyze expression. Gene Ontology analysis was performed using the GORILLA platform.

*ChIP-seq*—Chromatin and protein complexes from $1.5 \times 10^7$ ST2 cells were cross-linked for 10 min in 1% formaldehyde and flash-frozen. Chromatin was sonicated to an average size of 200–450 bp using a Sonics Vibracell sonicator (model Vcx 500). Chromatin complexes were immunoprecipitated using antibodies that recognized the histone modifications H3K9ac (Millipore 17–658) and H3K4me3 (Millipore CS200580). ChIP DNA was purified with the PCR purification kit (Qiagen),

**TABLE 2**
**PCR primers used in this study**

| Gene symbol | Forward | Reverse |
|---|---|---|
| *18s* | CGGCTACCACATCCAAGGAA | GCTGGAATTACCGCGGCT |
| *Alpl* | CCAACTCTTTTGTGCCAGAGA | GGCTACATTGGTGTTGAGCTTTT |
| *Ibsp* | CAGAGGAGGCAAGCGTCACT | GCTGTCTGGGTGCCAACACT |
| *Catnnb1* | CCTCCCAAGTCCTTTATGAATGG | CCGTCAATATCAGCTACTTGCTCTT |
| *Pparg* | GGAAAGACAACGGACAAATCAC | TACGGATCGAAACTGGCAC |
| *Cebpa* | TGAACAAGAACAGCAACGAG | TCACTGGTCACCTCCAGCAC |
| *Sp7* | CCCTTCTCAAGCACCAATGG | AAGGGTGGGTAGTCATTTGCATA |
| *ID2* | ATGAAAGCCTTCAGTCCGGTG | AGCAGACTCATCGGGTCGT |
| *Sox9* | CGGCTCCAGCAAGAACAAG | TGCGCCCACACCATGA |
| *Sox5* | TTTTCCCAACAAGCCTCACTC | TTGCCATCGACTTCCATTGTG |
| *Lef1* | CCTACAGCGACGAGCACTTTT | CCTTGCTTGGAGTTGACATCTG |
| *Bglap* | CAGCGGCCCTGAGTCTGA | GCCGGAGTCTGTTCACTACCTTA |
| *Pdk1* | AGGCGTTTATCCCCCGATTC | CGTAACCAAACCCAGCCAGG |

blunt-ended, and ligated to the sequencing adapters. The fragments were size-selected to 200–500 base pairs and underwent PCR amplification for 15 cycles. The resulting libraries were sequenced using the Illumina HiSeq-2000 as single reads extending 42 bases. The raw data were demultiplexed and aligned to the reference genome (mm9) using Bowtie. MACS was used for peak calling and generation of Wiggle plots. Transcription start site enrichment, meta-gene analysis, and heatmaps were generated using Cistrome.

*Western Blotting*—ST2 cells were scraped in lysis buffer containing 50 mM Tris (pH 7.4), 15 mM NaCl, 0.5% Nonidet P-40, and a protease inhibitor mix (Roche Applied Science #04693124001). Protein concentration was estimated by the BCA method (Pierce). Protein (20 $\mu$g) was resolved on 12% polyacrylamide gel and subjected to immunoblot analysis using the respective antibodies. Prestained dual color protein standards were used as molecular weight markers (Bio-Rad). After protein transfer, the blots were typically cut into multiple strips according to the molecular weight markers so that proteins of different sizes could be detected simultaneously from the same blot. Antibodies against Acly (Cell Signaling #4332, 1:1000 dilution) and $\beta$-actin (Cell Signaling #4970, 1:1000 dilution) were used to detect the respective protein levels. The immunoblots were blocked for 1 h at room temperature in 5% BSA (TBS, 0.1% Tween) followed by an overnight incubation at 4 °C in their respective diluted primary antibody solutions. Membranes were then washed three times using TBS/Tween 0.1% and further incubated with the secondary antibody, HRP goat anti-rabbit (Invitrogen, catalogue no. G21234) in 5% BSA (TBS/Tween 0.1%) for 1 h at room temperature (1:5000). All blots were developed using either the Immun-Star WesternC Chemiluminescence kit or the Clarity ECL substrate (Bio-Rad). Each experiment was repeated for a minimum of three times with three independently prepared protein samples.

*Acid Extraction of Histones*—For the analysis of histone modifications, histones were acid-extracted as described (36). Briefly, cells were trypsinized, washed, and incubated in hypotonic lysis buffer (10 mM Tris pH 8, 1 mM KCl, 1.5 mM $MgCl_2$, 1 mM DTT) for 30 min, and the nuclei were pelleted at 3000 $\times$ *g* for 5 min at 4 °C. Nuclei were resuspended in 4% $H_2SO_4$ and protein was pelleted at 15,000 $\times$ *g* for 10 min. Histones were precipitated with 33% trifluoroacetic acid (v/v), washed 2$\times$ with acetone, dried, and resuspended in deionized water. Histones were quantified using the BCA method and confirmed by Coomassie staining. Histones (1 $\mu$g) were resolved on a 15% acrylamide gel and blotted with antibodies that recognized the following modifications: H3K9/14ac (Cell Signaling #9677), acetylated H3 (Millipore 06-599), H3K9ac (Millipore 17-658), H4K12ac (Millipore 07-595), total H3 (Abcam ab1791), H3K9me3 (Millipore 17-625), H3K36me3 (Abcam ab9050), H3K27me3 (Abcam ab6002), H3K79me3 (Abcam ab2621), and H3K79me2 (Abcam ab3594). All primary antibodies were used at 1:1000 dilutions. Loading of histones was monitored by Coomassie staining and by detection of total H3 levels. Western blot signals were quantified using Image J software. Each experiment was done a minimum of three times with three independently prepared protein samples.

*Acetyl-CoA Extraction*—For the extraction of acetyl-CoA, 12–15 $\times$ $10^7$ cells were trypsinized, washed, and incubated in hypotonic lysis buffer for 30 min, and the nuclei were pelleted at 3000 $\times$ *g* for 5 min at 4 °C. Nuclei were resuspended in 10% trichloroacetic acid (Sigma). 100 ng of propionyl-CoA (Sigma) standard was added, and the nuclei were sonicated at 20% amplitude for 30 s and centrifuged at 15,000 $\times$ *g* for 5 min at 4 °C to precipitate the protein pellet. The nuclear lysate was bound to an HLB Oasis 3cc column, washed, and eluted in 600 $\mu$l of methanol.

*Acetyl-CoA Quantification by Mass Spectrometry*—HPLC mass spectrometric analysis of acetyl-CoA was conducted on a Thermo Finnigan (San Jose, CA) TSQ Vantage triple-stage quadrupole instrument with Thermo Accela UPLC operated with Xcalibur software. Lipid extracts with propyl-CoA internal standard were injected with a Thermo Accela autosampler and separated with a Thermo BETASIL C18 reversed-phase column (100 $\times$ 2.1 mm; 3-$\mu$m particle size) coupled to the electrospray ionization source, where the skimmer was set at ground potential, the electrospray needle was set at 4.0 kV, and temperature of the heated capillary was 300 °C. Tandem mass spectrometry was operated in the negative-ion mode in which precursor-ion scan of *m*/*z* 134.1 with a collision energy of 21 V was employed. The tandem quadrupole mass spectra were acquired in the profile mode in the mass range of 390–420 Da with a scan rate of 1 scan/s for detection of the acyl-CoA as the $[M-2H]^{2-}$ ions. The mass resolution of the instrument was tuned to 0.6 Da at half-peak height.

HPLC separation was carried out with a step gradient in which mobile phase A was 5% acetonitrile in water with 0.1% $NH_4OH$ and mobile phase B was 0.1% $NH_4OH$ in 95% acetoni-

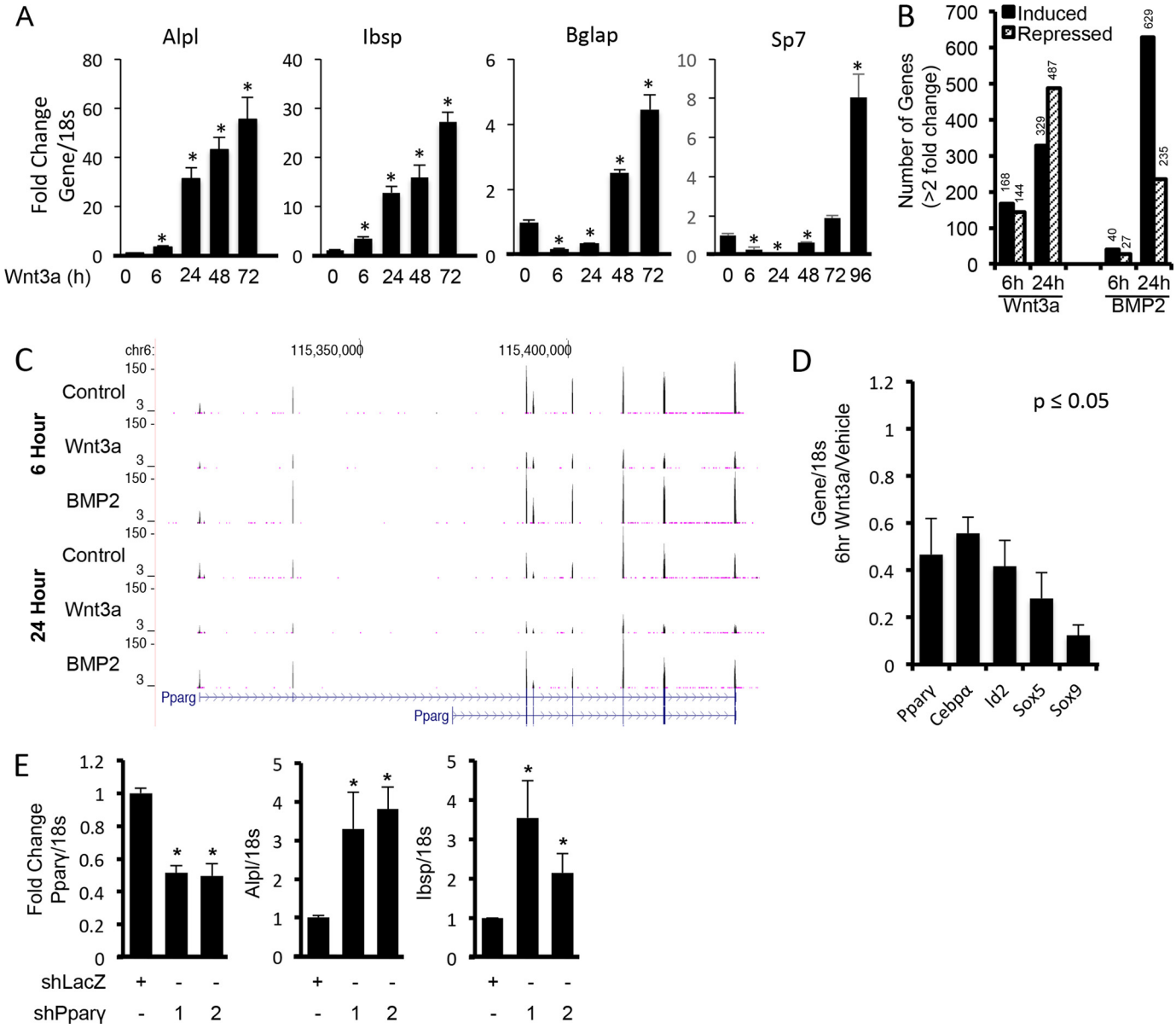


FIGURE 1. **Wnt3a suppresses gene expression in ST2 cells.** *A*, qPCR analyses of the effect of Wnt3a treatment on osteoblast marker gene induction in ST2 cells. *B*, total number of genes induced or suppressed (>2-fold) by Wnt3a or BMP2 after 6 or 24 h of treatment, as detected by RNA-seq. *C*, alignment of mapped sequence reads to *Pparg* locus treated with vehicle (*Control*), Wnt3a, or BMP2 for either 6 or 24 h. *D*, qPCR confirmation of gene suppression in response to 6 h of Wnt3a treatment. *E*, qPCR analyses of the effect of *Pparg* knockdown by shRNA on osteoblast marker gene induction in ST2 cells. Two different shRNAs were used for *Pparg* (1 and 2); shLacZ was the negative control. *, $p < 0.05$, $n = 3$. *Error bars*: S.D.

trile/water. Step gradient elution was performed with an initial condition of 100% A for 4 min and switched to mobile phase B for an additional 4 min. The column was then re-equilibrated at 100% B for 10 min before subsequent injections. The flow rate was 50 $\mu$l/min at ambient temperature.

*Nuclear Citrate Measurement*—Nuclear citrate concentration was measured using the citrate fluorometric assay kit (Sigma, MAK057). For the extraction of citrate, nuclei from ST2 cells treated with L- or Wnt3a-conditioned media were resuspended in 0.1 ml of citrate assay buffer. Insoluble material was removed by centrifugation at 15,000 × *g* for 10 min at 4 °C. Nuclear supernatants were concentrated on 10-kDa spin columns (Abcam ab93349) at 10,000 × *g* for 20 min. 25 $\mu$l of nuclear extract was used for each technical replicate. Citrate concentration was extrapolated from a standard curve and normalized to cell number. Each assay was performed in technical duplicate from six independent experiments.

*$CO_2$ Trap Experiments*—The procedure is as described previously (37). Briefly, ST2 cells were seeded at $4 \times 10^5$/flask and cultured in media containing 2 $\mu$l of 0.1 mCi/ml $^{14}$C-labeled glucose (total radioactivity 444,000 dpm) with or without Wnt3a (100 ng/ml) in the sealed $CO_2$ trap system for 24 h before $CO_2$ was harvested for the measurement of radioactivity. [3,4-$^{14}C_2$]Glucose (catalog #ARC 0211A) and [6-$^{14}$C]glucose-(catalog #ARC 0121B) were from American Radiolabeled Chemicals (St. Louis, MO). A parallel experiment was conducted with identical treatments for cell counting. For glucose

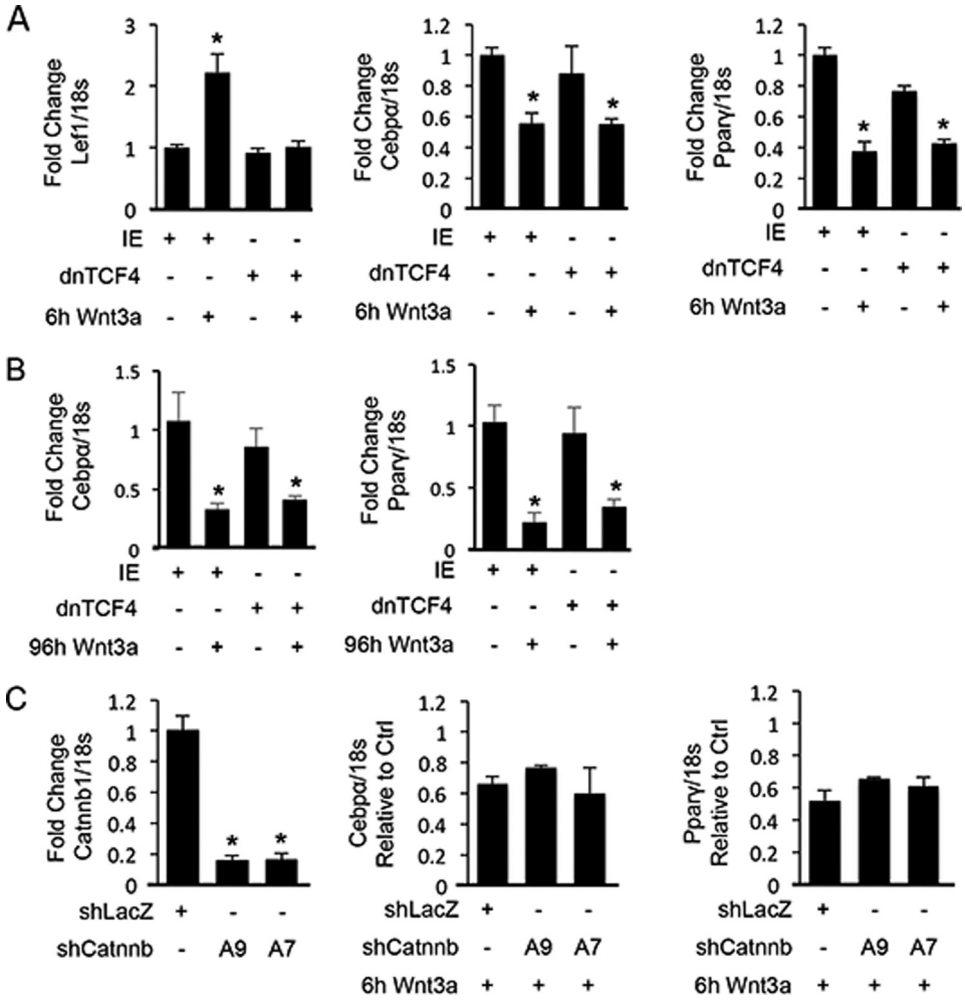


FIGURE 2. **Wnt-induced gene suppression is independent of β-catenin signaling.** *A* and *B*, qPCR analyses of the effect of viral expression of dnTCF4 on gene suppression in response to Wnt3a after 6 h (*A*) or 96 h(*B*). *C*, qPCR analyses of the effect of β-catenin knockdown on Wnt3a-induced gene suppression. *IE*, control retrovirus expressing EGFP. Two shRNAs are used against β-catenin (shCatnnb-A7 and -A9).

consumption, an aliquot of the medium was taken for measurements before the injection of $H_2SO_4$.

## Results

*Wnt3a Acutely Suppresses Gene Expression*—To investigate how Wnt signaling induces osteoblast differentiation, we applied Wnt3a to ST2 cells, a progenitor cell that possesses both osteogenic and adipogenic potential but undergoes osteoblast differentiation in response to Wnt3a (13, 38, 39). Wnt3a-induced osteoblast differentiation was confirmed by the time-dependent up-regulation of marker genes such as Alpl, Ibsp, Bglap, and Sp7 (Fig. 1*A*). Interestingly, Sp7 and Bglap were initially suppressed by Wnt3a before being up-regulated at the later time points. To gain insights about the early transcriptional response to Wnt3a, we profiled the transcriptome by RNA-seq in these cells after 6 and 24 h of treatment. For comparison, we conducted similar experiments with BMP2, another potent osteogenic signal for ST2 cells. Unexpectedly, Wnt3a suppressed the mRNA levels of a large number of genes as early as 6 h of treatment (144 genes with >2-fold decrease), and the number of suppressed genes surpassed those induced at 24 h (487 *versus* 329 genes, with a >2-fold change) (Fig. 1*B*). In contrast, BMP2 altered the expression of much fewer genes at 6 h, and the number of genes suppressed was considerably lower than those induced at both 6 and 24 h (Fig. 1*B*). The prominent feature of gene suppression by Wnt3a was unexpected, as gene activation through β-catenin is presumed to be the dominant mode of Wnt3a signaling. We performed gene ontology (GO) analysis of genes suppressed at least 2-fold by Wnt3a using GOrilla (40). This analysis revealed that the suppressed transcripts were significantly enriched for genes involved in "positive regulation of cell differentiation" (GO: 0045597, $p = 7.22E^{-10}$) and "positive regulation of transcription, DNA-dependent" (GO:0045893, $p = 1.87E^{-06}$). These genetic cadres include transcription factors known to regulate the differentiation of adipocytes (*e.g. Pparg*, *Cebpa*, and *Id2*) and chondrocytes (*e.g. Sox5* and *Sox9*) (see Fig. 1*C* for the RNA-seq alignment for the representative gene *Pparg*). With quantitative PCR, we confirmed that these adipogenic or chondrogenic transcription factors were all suppressed upon 6 h of Wnt3a treatment (Fig. 1*D*). Like recombinant Wnt3a, virally expressed Wnt10b or Wnt7b, both known to induce osteoblast differentiation, caused similar suppression of those genes (data not shown). Others have also observed the suppressive effect of

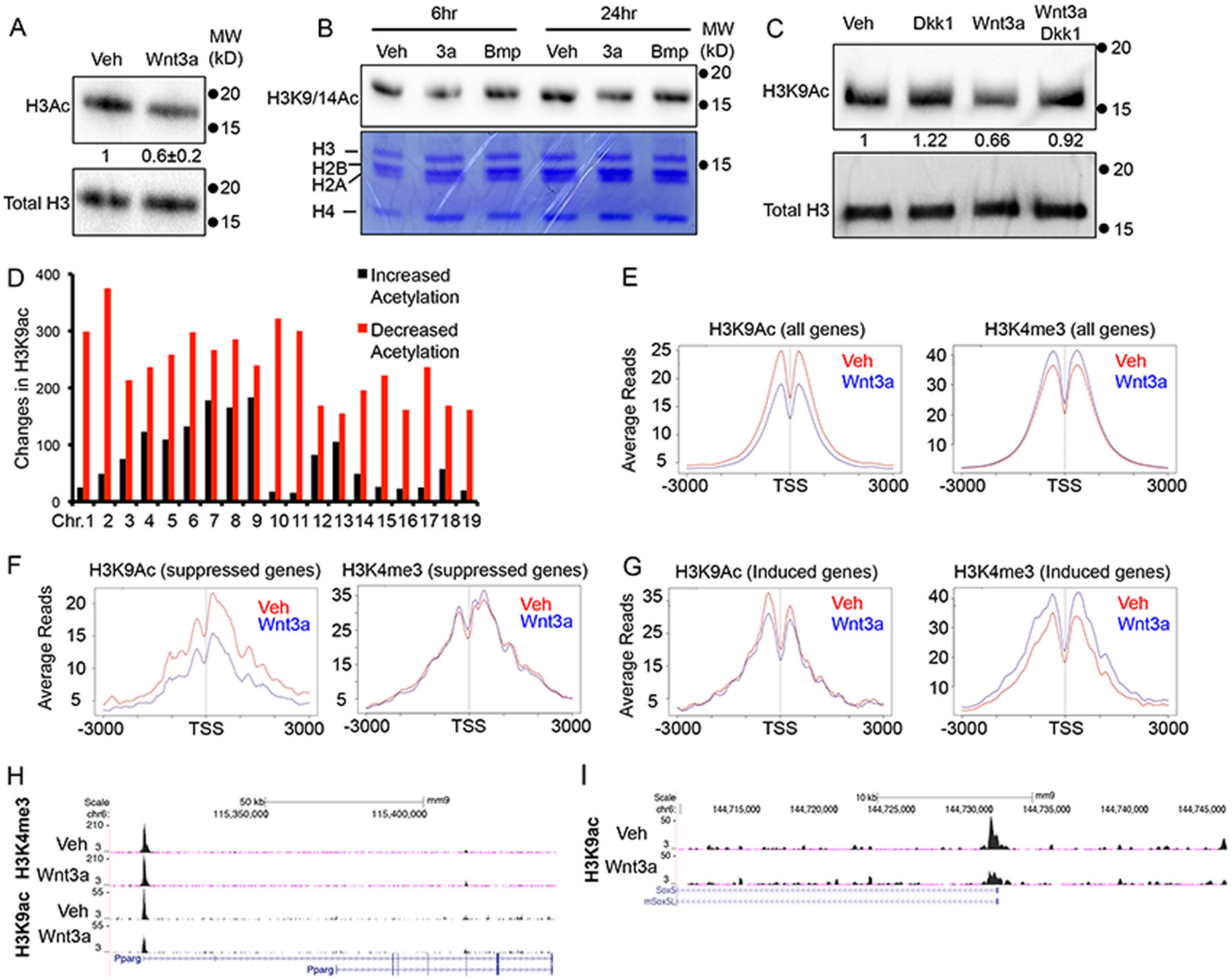


FIGURE 3. **Decrease in histone acetylation correlates with gene suppression.** *A–C*, Western blot analyses of acid extracted histones after 6 h Wnt3a treatment (*A* and *C*) or after 6 or 24 h of Wnt3a or BMP2 treatment in ST2 cells (*B*). *Veh*, vehicle. Acetylated H3 was normalized to total H3 in *A* and *C*. Data are -fold change ± S.D. for Wnt3a over vehicle in three independent experiments in A. Coomassie staining of acid-extracted histones is shown in *B*. Quantification is shown for a representative blot in *C*. Note different positioning of size markers from that in other blots due to the use of a gradient gel in C. *D*, ChIP-seq data showing the number of genomic loci with called peaks for increased *versus* decreased H3K9ac, on each autosome. *E–G*, ChIP-seq data showing average H3K9ac or H3K4me3 reads at the promoter regions of all (*E*), suppressed (*F*), or induced (*G*) genes. *H* and *I*, H3K4me3 and/or H3K9ac profiles at the promoter region of Pparg (*H*) or Sox5 (*I*), both suppressed by Wnt3a.

Wnt10b on *Pparg* and *Cebpa* and further demonstrated that knockdown of *Pparg* or *Cebpa* induced spontaneous osteoblast differentiation in ST2 cells (38). We confirmed that *Pparg* knockdown (by ~50%) alone was sufficient to induce the expression of osteoblast markers *Alpl* and *Ibsp*, albeit less efficiently than Wnt3a (Fig. 1*E*). In contrast to Wnt, BMP2 did not suppress *Pparg* or *Cebpa* nor did it impair adipocyte differentiation in ST2 cells (data not shown). Thus, unlike BMP, Wnt appears to induce osteoblast differentiation in part through suppression of adipogenic transcription factors and the alternative cell fate.

*Wnt3a Acutely Reduces Histone Acetylation*—To investigate the mechanism of gene suppression by Wnt3a, we first evaluated if β-catenin-mediated transcription was required. Expression of a dnTCF4 completely abrogated the induction of β-catenin target genes like *Lef1* by Wnt3a but had no effect on the suppression of *Pparg* or *Cebpa* at either 6 or 96 h of Wnt treatment (Fig. 2, *A* and *B*). Similarly, knockdown of β-catenin had no effect on Wnt3a-dependent suppression (Fig. 2*C*). These results are consistent with the fact that Wnt7b suppressed gene expression even though it did not activate β-catenin-dependent gene transcription in ST2 cells (13). Thus, gene suppression in response to Wnt3a is unlikely to be secondary to gene activation mediated by the β-catenin·Tcf complex.

Because histone acetylation and methylation are associated with gene transcription, we next evaluated the effect of Wnt3a on such modifications of bulk histones. Remarkably, after 6 h of treatment, Wnt3a reduced the acetylation of histone H3, a modification associated with active gene transcription, and the effect lasted for at least 24 h (Fig. 3, *A* and *B*). In contrast, BMP2 did not suppress histone acetylation (Fig. 3*B*). The suppression of histone acetylation by Wnt3a likely required Lrp5/6 signal-

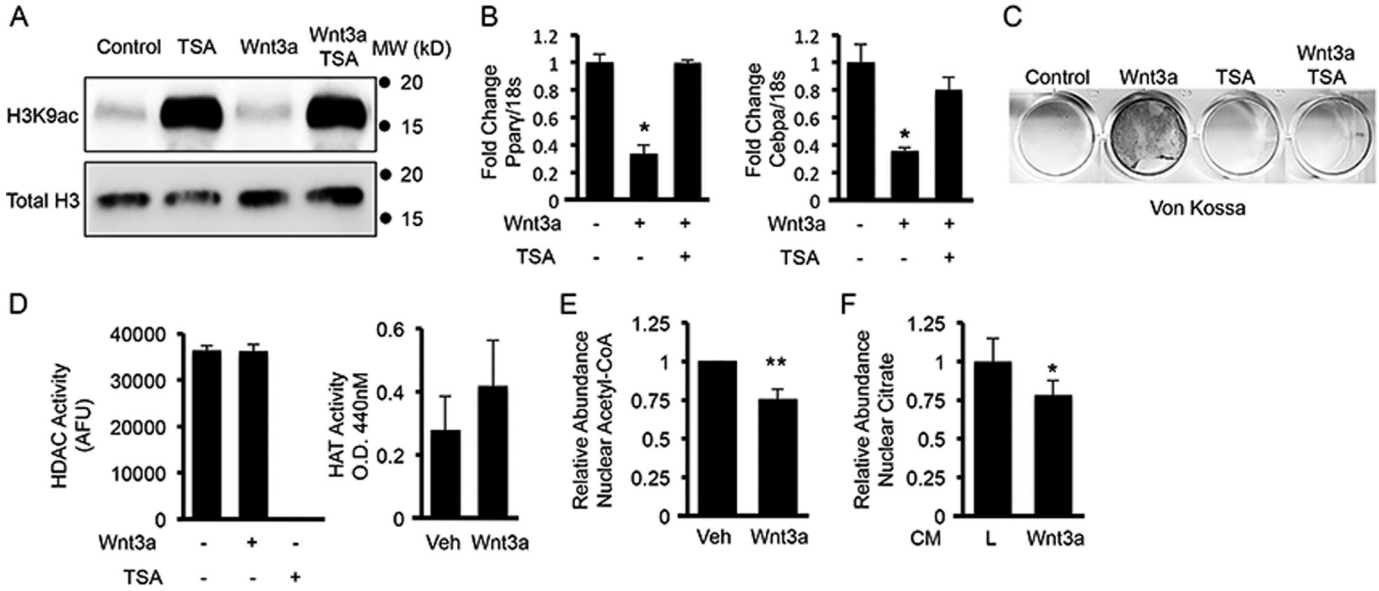


FIGURE 4. **Wnt decreases nuclear acetyl-CoA and citrate levels to reduce histone acetylation.** *A–C*, effects of TSA on histone acetylation (*A*), gene suppression (*B*), and matrix mineralization (*C*) in response to Wnt3a. *, $p < 0.05$, $n = 3$. *D*, HDAC or HAT activity assay performed with nuclear extracts from ST2 cells treated with vehicle or Wnt3a for 6 h. Cells treated with TSA were used as a control for HDAC activity assay. *AFU,* arbitrary fluorescence units. *E*, effect of Wnt3a on nuclear acetyl-CoA levels. Acetyl-CoA abundance was normalized to 100 ng of propionyl-CoA added to the nuclear extract as an internal standard. **, $p = 0.004$, $n = 5$. *F*, effect of Wnt3a on nuclear citrate levels. *, $p = 0.015$, $n = 6$. *Wnt3a*, L cells expressing Wnt3a. *Error bars*: S.D.

ing as Dkk1, which is known to interfere with the Wnt-Lrp5/6 interaction, notably diminished the effect (Fig. 3*C*). A survey of several histone methylation marks indicated that Wnt3a did not alter the levels of H3K9me3, H3K27me3, H3K4me3, or H3K36me3, although it increased H3K79me3, likely due to the methyltransferase activity of the β-catenin·Dot complex induced by Wnt signaling as previously reported (19, 21). Thus, Wnt signaling acutely reduces histone acetylation, and this event may account for the rapid suppression of gene expression.

We next sought to determine whether the decrease in bulk histone acetylation was reflected by changes on the chromatin. For this, we performed chromatin Immunoprecipitation followed by deep sequencing (ChIP-Seq) using antibodies specific for acetylated H3K9 (H3K9ac) or tri-methylated H3K4 (H3K4me3) to localize these modifications to particular loci on the chromatin. These experiments yielded 4565 genomic loci with decreased H3K9ac compared with only 1461 with increased H3K9ac after 6 h of Wnt3a stimulation. When examined individually, each autosome contained many more loci with decreased than increased H3K9ac (Fig. 3*D*). In contrast, Wnt3a only minimally affected H3K4me3, with 162 genomic loci showing an increase compared with 141 loci with a decrease. More importantly, all promoter regions (defined as ±3 kb flanking the transcription start site) in the genome on average exhibited a decrease in H3K9ac but a slight increase in H3K4me3 (Fig. 3*E*). When the promoter regions of all suppressed *versus* induced genes were analyzed separately, we saw that Wnt3a caused a decrease in H3K9ac in the former but an increase in H3K4me3 in the later (Fig. 3, *F* and *G*). Finally, 355 of the 4655 loci with decreased H3K9ac were located within 3 kb of a transcription start site and showed significant correlation with gene suppression ($p = 2.25 \times 10^{-23}$, hypergeometric test), as exemplified by *Pparg* and *Sox5* (Fig. 3, *H* and *I*). Conversely, Wnt3a-induced genes significantly overlapped with genes exhibiting increased H3K9ac in their promoters ($p = 0.00067$, hypergeometric test). There was no overlap between genes with decreased H3K9ac in the promoter and genes induced or vice versa. Thus, Wnt3a induces a genome-wide reduction in histone acetylation that correlates with broad gene suppression.

*Wnt3a Decreases Nuclear Acetyl-CoA and Citrate Levels*—To determine if decreased histone acetylation was required for gene suppression by Wnt signaling, we used trichostatin A (TSA) to inhibit both class I and II HDACs. TSA greatly increased histone acetylation in ST2 cells regardless of Wnt3a (Fig. 4*A*). Importantly, preventing histone deacetylation with TSA completely abolished Wnt3a-induced suppression of *Pparg* and *Cebpa* as well as osteoblast differentiation assayed by von Kossa staining (Fig. 4, *B* and *C*).

We next investigated how Wnt3a decreases histone acetylation. We found no change in either HDAC or HAT activities in assays with nuclear extracts after 6 h of Wnt3a treatment (Fig. 4*D*). Therefore, we hypothesized that Wnt3a suppressed histone acetylation by decreasing available acetyl-CoA, the substrate for HAT. We directly measured acetyl-CoA levels with mass spectrometry in nuclear extracts prepared from ST2 cells. These experiments revealed that Wnt3a reduced nuclear acetyl-CoA levels by 25% after 6 h of treatment (Fig. 4*E*). Thus, Wnt3a suppresses histone acetylation and gene expression likely by reducing nuclear acetyl-CoA levels.

Because citrate is the precursor for acetyl-CoA, we next examined the potential effect of Wnt3a on citrate levels in the nucleus. For this, we measured citrate levels in nuclear extracts prepared from ST2 cells treated with Wnt3a-conditioned media (Wnt3a-CM) or the control media. Wnt3a-CM reduced nuclear citrate levels by 24% after 6 h of treatment (Fig. 4*F*). Thus, Wnt3a appears to reduce the nuclear acetyl-CoA concentration by suppressing citrate levels.

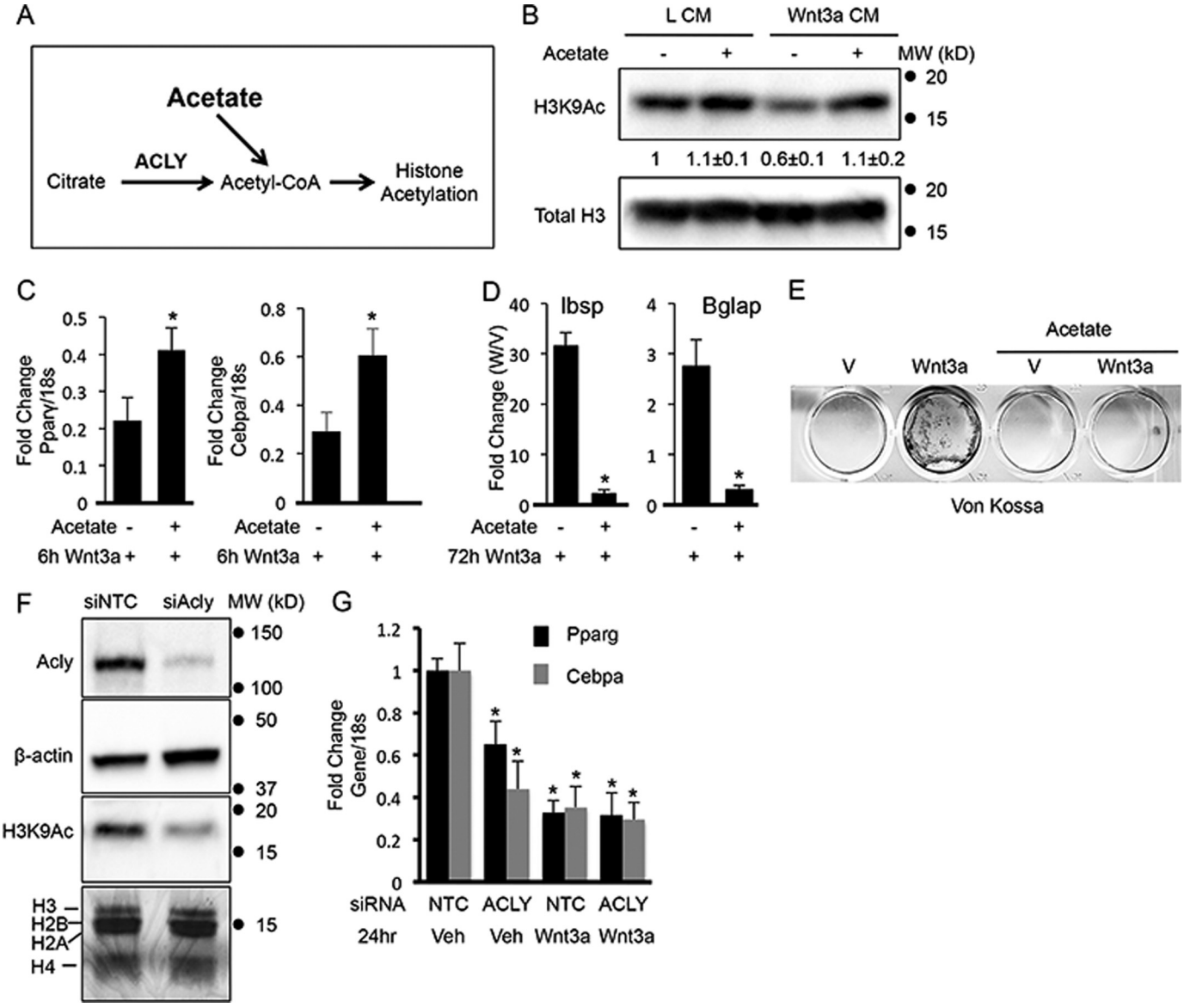


FIGURE 5. **Changes in acetyl-CoA production affect histone acetylation and gene expression.** *A*, schematic for acetyl-CoA production from citrate or acetate. Acly converts citrate into acetyl-CoA for histone acetylation. Acetate is converted into acetyl-CoA independent of citrate. *B*, effects of sodium acetate on H3K9ac in ST2 cells treated with Wnt3a- or L-cell CM for 6 h. Propionic acid was used as the negative control. H3K9ac was normalized to total H3. Data are -fold change ± S.D. from three independent experiments. *C–E*, effects of sodium acetate on Wnt3a-induced gene suppression at 6 h (*C*), osteoblast differentiation at 72 h (*D*), or matrix mineralization (*E*). *F* and *G*, effects of Acly knockdown (*siAcly*) on histone H3K9ac (*F*) or gene expression with or without Wnt3a treatment (*G*). *siNTC*, non-targeting control siRNA. Coomassie staining shows equal loading of acid-extracted histones in F. *, $p < 0.05$, $n = 3$. *Error bars*: S.D.

*Changes in Acetyl-CoA Production Affect Histone Acetylation and Gene Expression*—Our findings so far predict that changing nucleocytoplasmic acetyl-CoA levels would affect Wnt3a-induced histone deacetylation and gene suppression. To test this prediction, we treated ST2 cells with supraphysiological levels of acetate, which is converted to acetyl-CoA by ACECS1 and expected to elevate nucleocytoplasmic acetyl-CoA levels (Fig. 5*A*) (5). Acetate by itself slightly increased H3K9ac and completely reversed the effect of Wnt3a on histone acetylation (Fig. 5*B*). Importantly, acetate not only blunted the suppression of *Pparg* and *Cebpa* by Wnt3a but also impaired Wnt3a-induced osteoblast differentiation as assayed by both gene expression and von Kossa staining (Fig. 5, *C–E*). We next used siRNA to knock down Acly, the principle enzyme responsible for generating nucleocytoplasmic acetyl-CoA from citrate in mammalian cells (Fig. 5*A*) (5). Acly knockdown, similar to Wnt3a, markedly decreased H3K9ac levels and suppressed Pparg and Cebpa expression, but Wnt3a and Acly knockdown did not have an additive effect on gene suppression (Fig. 5, *F* and *G*). These results further support the conclusion that Wnt3a suppresses histone acetylation by reducing acetyl-CoA levels.

*Wnt3a Suppresses Glucose Entry to TCA Cycle to Reduce Histone Acetylation*—Glucose oxidation in the TCA cycle is a primary source of citrate for acetyl-CoA production, and we have previously shown that Wnt signaling stimulates glucose consumption and lactate production from glucose (5, 41). To examine directly the effect of Wnt on glucose oxidation through the TCA cycle, we used a $CO_2$ trapping method to

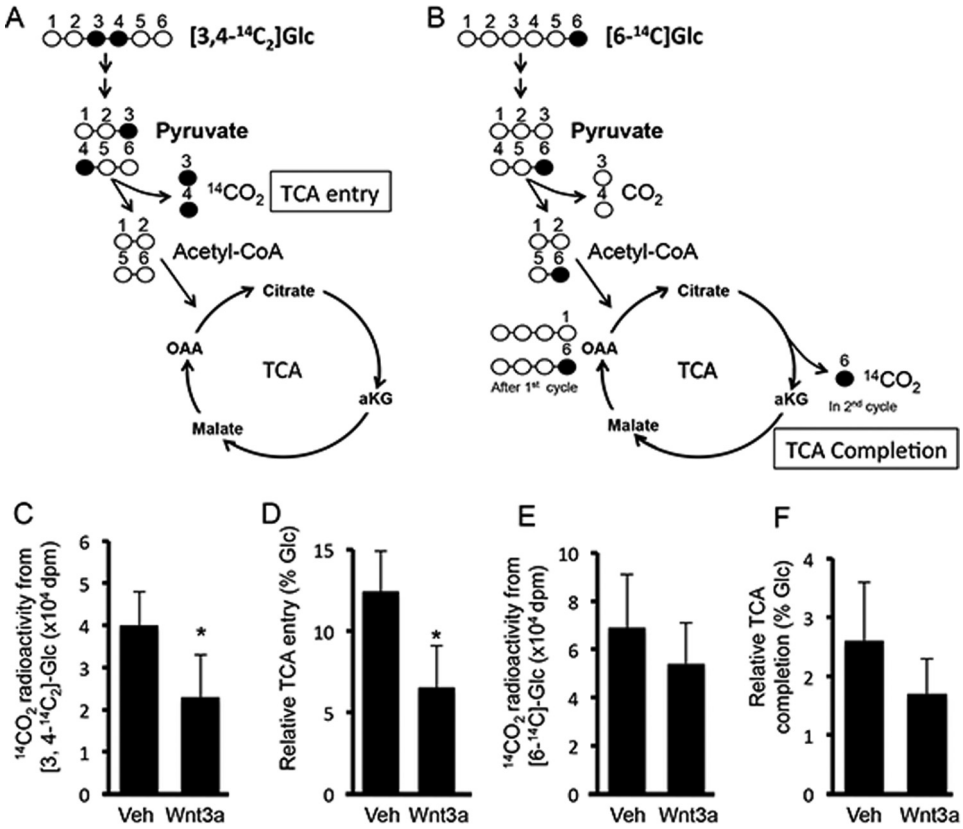


FIGURE 6. **Wnt suppresses glucose entry into TCA cycle.** *A* and *B*, graphic depiction of $CO_2$ generation from glucose labeled with $^{14}C$ at specific positions. The *black circle* denotes labeled carbon. The *white circle* denotes unlabeled carbon. *OAA,* oxaloacetate; *aKG,* α-ketoglutarate. *C–F*, $^{14}CO_2$ production from [3,4-$^{14}C_2$]glucose (*C* and *D*) or [6-$^{14}C$]glucose (*E* and *F*) in ST2 cells treated with Wnt3a or vehicle (*Veh*) for 24 h. *, $p < 0.05$ $n = 5$. *Error bars:* S.D.

capture radioactive $^{14}CO_2$ produced from glucose labeled with $^{14}C$ at specific positions. In this method, [3,4-$^{14}C_2$]glucose produces $^{14}CO_2$ upon entry into the TCA cycle via conversion of pyruvate into acetyl-CoA and $^{14}CO_2$ (Fig. 6*A*). On the other hand, [6-$^{14}C$]glucose produces $^{14}CO_2$ during the conversion of citrate to α-ketoglutarate after completion of the first round of the TCA cycle (Fig. 6*B*). Despite a greater amount of total glucose consumption, the cells treated with Wnt3a released significantly less $^{14}CO_2$ from [3,4-$^{14}C_2$]glucose than the control (Fig. 6*C*). Upon normalized to glucose consumption, the percentage of glucose entering the TCA cycle was reduced by nearly 50% by Wnt3a over the control (Fig. 6*D*). On the other hand, the amount of glucose that completes the TCA cycle, as measured by $^{14}CO_2$ radioactivity released from [6-$^{14}C$]glucose, was not affected by Wnt3a (Fig. 6, *E* and *F*). Thus, Wnt signaling reduces the amount of glucose entering the TCA cycle, and this may be responsible for the decrease of citrate and acetyl-CoA levels in the nucleus.

Our data predict that reducing glucose entry into the TCA cycle should mimic the effect of Wnt3a on histone acetylation. As a proof of principle, withdrawal of glucose from the culture media for 12 h markedly decreased histone acetylation in ST2 cells (Fig. 7*A*). We next tested whether preventing glucose metabolism into the TCA cycle was sufficient to decrease histone acetylation in the absence of Wnt signaling. Specifically, we overexpressed Pdk1, which phosphorylates and inhibits pyruvate dehydrogenase, thus preventing pyruvate oxidation and entry into the TCA cycle (Fig. 7*B*). Pdk1 overexpression not only reduced histone acetylation by 47% but also suppressed gene expression of *Pparg* and *Cebpa* in ST2 cells (Fig. 7, *C* and *D*). Thus, Wnt signaling suppresses histone acetylation likely through reprogramming of glucose metabolism.

## Discussion

We have provided evidence that Wnt signaling induces osteoblast differentiation in part through epigenetic suppression of gene expression. The data support the mechanism that Wnt3a acutely reprograms glucose metabolism to reduce the nuclear level of citrate and acetyl-CoA, resulting in a decrease in histone acetylation independent of β-catenin. The current study expands our understanding about how Wnt regulates gene expression.

The study provides a mechanistic link between reduced TCA metabolism of glucose and the early phase of osteoblast differentiation in response to Wnt. Our finding is reminiscent of a recent report that decreased glycolysis reduces acetyl-CoA and histone acetylation during early differentiation of embryonic stem cells (42). Thus, a glycolytic switch appears to trigger cellular differentiation in multiple settings.

Our study reveals that Wnt signaling induces osteoblast differentiation in part through epigenetic suppression of transcription factors specifying the alternative fate of adipocyte. In contrast, BMP2 does not utilize the same mechanism but rather induces the expression of Sp7, an osteogenic transcription factor. Thus, in ST2 cells, Wnt3a and BMP2 induce osteoblast differentiation through apparently different mechanisms. It

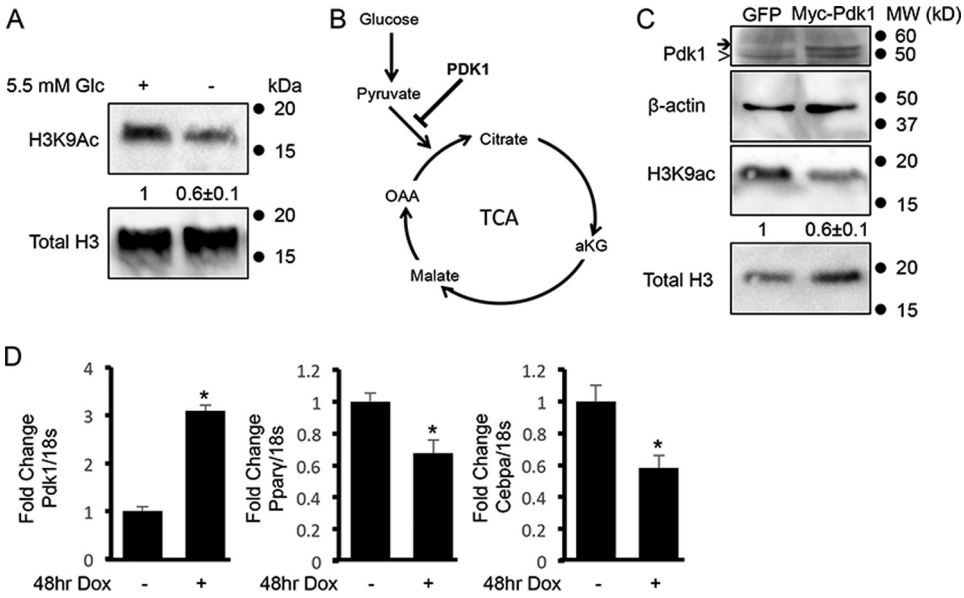


FIGURE 7. **Suppression of glucose metabolism reduces histone acetylation.** *A*, Western blot analyses of acid extracted histones in ST2 cells cultured for 12 h in the presence or absence of 5. 5 mM glucose. Acetylated H3K9 was normalized to total H3. Data are -fold change ± S.D. from three independent experiments. *B*, diagram of glucose oxidation through the TCA cycle. *OAA*, oxaloacetate; *aKG*, α-ketoglutarate. *C*, effect of myc-Pdk1 expression on H3K9 acetylation in ST2 cells. GFP or myc-Pdk1 was expressed from lentiviral vectors in response to doxycycline. GFP is a negative control. The *arrow* denotes myc-Pdk1; the *arrowhead* denotes endogenous Pdk1. H3K9ac was normalized to total H3. Data are -fold change ± S.D. from three independent experiments. *D*, effect of myc-Pdk1 expression on gene expression in ST2 cells infected with lentiviruses with or without doxycycline (*Dox*) treatment. *, $p < 0.05$, $n = 3$. *Error bars*: S.D.

should be noted that β-catenin is also necessary for Wnt3a-induced osteoblast differentiation in ST2 cells as knockdown of β-catenin essentially abolished the induction of *Alpl*. Thus, WNT signaling induces osteoblast differentiation both by gene activation via β-catenin and by gene suppression through acetyl-CoA-mediated epigenetic regulation.

Our findings may have broad implications for understanding epigenetic regulations of gene expression. The prevailing view holds that epigenetic changes require *de novo* binding of transcription factors to specific DNA sequences, which subsequently recruit chromatin-modifying enzymes. Our results, however, indicate that developmental signals can act through intermediate metabolites to alter chromatin modifications and gene expression. The acute response in the level of histone acetylation likely reflects the dynamic nature of acetylation *versus* deacetylation on the genomic loci already occupied by the respective enzymes. Although our *in vitro* assays did not detect any change in total Hdac or Hat activity in nuclear extracts in response to Wnt3a, the results do not exclude the possibility that the enzymatic activity might be altered *in vivo*. Indeed, a recent study has linked decreased intracellular pH with global histone deacetylation (43). Considering our previous finding that Wnt signaling stimulates lactate production from glucose, it is conceivable that a lower intracellular pH could result and also contribute to histone deacetylation (41). Although previous studies have shown that chromatin acetylation decreased with differentiation of embryonic stem cells, they did not demonstrate a causal relationship between deacetylation and differentiation (44). Interestingly, Acly knockdown induces differentiation in C2C12 myoblasts but does not affect differentiation of 3T3L1 preadipocytes even though it prevents lipid accumulation, indicating that modulation of acetyl-CoA levels likely has a context-dependent role during differentiation (5, 45). Finally, the present study raises the possibility that other substrates or co-factors for chromatin-modifying enzymes may also respond to physiological signals in a biologically meaningful way to affect gene expression.

*Author Contributions*—C. M. K., E. E., and J. C. conducted most of the experiments. F.-F H. and J. T. performed mass spectrometric measurements of acetyl-CoA. F. L. conceived then idea for the project. C. M. K. and F. L. analyzed the data and wrote the paper.

*Acknowledgment—We thank Paul Cliften (Washington University School of Medicine) for help with MACS and bioinformatics.*

## References

1. Goldberg, A. D., Allis, C. D., and Bernstein, E. (2007) Epigenetics: a landscape takes shape. *Cell* **128,** 635–638
2. Jenuwein, T., and Allis, C. D. (2001) Translating the histone code. *Science* **293,** 1074–1080
3. Kouzarides, T. (2007) Chromatin modifications and their function. *Cell* **128,** 693–705
4. Guarente, L. (2000) Sir2 links chromatin silencing, metabolism, and aging. *Genes Dev.* **14,** 1021–1026
5. Wellen, K. E., Hatzivassiliou, G., Sachdeva, U. M., Bui, T. V., Cross, J. R., and Thompson, C. B. (2009) ATP-citrate lyase links cellular metabolism to histone acetylation. *Science* **324,** 1076–1080
6. Tsukada, Y., Fang, J., Erdjument-Bromage, H., Warren, M. E., Borchers, C. H., Tempst, P., and Zhang, Y. (2006) Histone demethylation by a family of JmjC domain-containing proteins. *Nature* **439,** 811–816
7. Inoki, K., Ouyang, H., Zhu, T., Lindvall, C., Wang, Y., Zhang, X., Yang, Q., Bennett, C., Harada, Y., Stankunas, K., Wang, C. Y., He, X., MacDougald, O. A., You, M., Williams, B. O., and Guan, K. L. (2006) TSC2 integrates Wnt and energy signals via a coordinated phosphorylation by AMPK and GSK3 to regulate cell growth. *Cell* **126,** 955–968
8. Habas, R., Dawid, I. B., and He, X. (2003) Coactivation of Rac and Rho by Wnt/Frizzled signaling is required for vertebrate gastrulation. *Genes Dev.* **17,** 295–309

9. Habas, R., Kato, Y., and He, X. (2001) Wnt/Frizzled activation of Rho regulates vertebrate gastrulation and requires a novel Formin homology protein Daam1. *Cell* **107,** 843–854
10. Wu, X., Tu, X., Joeng, K. S., Hilton, M. J., Williams, D. A., and Long, F. (2008) Rac1 activation controls nuclear localization of β-catenin during canonical Wnt signaling. *Cell* **133,** 340–353
11. Kühl, M., Sheldahl, L. C., Park, M., Miller, J. R., and Moon, R. T. (2000) The Wnt/$Ca^{2+}$ pathway: a new vertebrate Wnt signaling pathway takes shape. *Trends Genet.* **16,** 279–283
12. Kinoshita, N., Iioka, H., Miyakoshi, A., and Ueno, N. (2003) PKCδ is essential for Dishevelled function in a noncanonical Wnt pathway that regulates *Xenopus* convergent extension movements. *Genes Dev.* **17,** 1663–1676
13. Tu, X., Joeng, K. S., Nakayama, K. I., Nakayama, K., Rajagopal, J., Carroll, T. J., McMahon, A. P., and Long, F. (2007) Noncanonical Wnt signaling through G protein-linked PKCδ activation promotes bone formation. *Dev. Cell* **12,** 113–127
14. Yoon, J. C., Ng, A., Kim, B. H., Bianco, A., Xavier, R. J., and Elledge, S. J. (2010) Wnt signaling regulates mitochondrial physiology and insulin sensitivity. *Genes Dev.* **24,** 1507–1518
15. Frey, J. L., Li, Z., Ellis, J. M., Zhang, Q., Farber, C. R., Aja, S., Wolfgang, M. J., Clemens, T. L., and Riddle, R. C. (2015) Wnt-Lrp5 signaling regulates fatty acid metabolism in the osteoblast. *Mol. Cell. Biol.* **35,** 1979–1991
16. Pate, K. T., Stringari, C., Sprowl-Tanio, S., Wang, K., TeSlaa, T., Hoverter, N. P., McQuade, M. M., Garner, C., Digman, M. A., Teitell, M. A., Edwards, R. A., Gratton, E., and Waterman, M. L. (2014) Wnt signaling directs a metabolic program of glycolysis and angiogenesis in colon cancer. *EMBO J.* **33,** 1454–1473
17. Karner, C. M., Esen, E., Okunade, A. L., Patterson, B. W., and Long, F. (2015) Increased glutamine catabolism mediates bone anabolism in response to WNT signaling. *J. Clin. Invest.* **125,** 551–562
18. Hecht, A., Vleminckx, K., Stemmler, M. P., van Roy, F., and Kemler, R. (2000) The p300/CBP acetyltransferases function as transcriptional coactivators of β-catenin in vertebrates. *EMBO J.* **19,** 1839–1850
19. Mohan, M., Herz, H. M., Takahashi, Y. H., Lin, C., Lai, K. C., Zhang, Y., Washburn, M. P., Florens, L., and Shilatifard, A. (2010) Linking H3K79 trimethylation to Wnt signaling through a novel Dot1-containing complex (DotCom). *Genes Dev.* **24,** 574–589
20. Sierra, J., Yoshida, T., Joazeiro, C. A., and Jones, K. A. (2006) The APC tumor suppressor counteracts β-catenin activation and H3K4 methylation at Wnt target genes. *Genes Dev.* **20,** 586–600
21. Mahmoudi, T., Boj, S. F., Hatzis, P., Li, V. S., Taouatas, N., Vries, R. G., Teunissen, H., Begthel, H., Korving, J., Mohammed, S., Heck, A. J., and Clevers, H. (2010) The leukemia-associated Mllt10/Af10-Dot1l are Tcf4/β-catenin coactivators essential for intestinal homeostasis. *PLoS Biol.* **8,** e1000539
22. Long, F. (2012) Building strong bones: molecular regulation of the osteoblast lineage. *Nat. Rev. Mol. Cell Biol* **13,** 27–38
23. Hu, H., Hilton, M. J., Tu, X., Yu, K., Ornitz, D. M., and Long, F. (2005) Sequential roles of Hedgehog and Wnt signaling in osteoblast development. *Development* **132,** 49–60
24. Day, T. F., Guo, X., Garrett-Beal, L., and Yang, Y. (2005) Wnt/β-catenin signaling in mesenchymal progenitors controls osteoblast and chondrocyte differentiation during vertebrate skeletogenesis. *Dev. Cell* **8,** 739–750
25. Hill, T. P., Später, D., Taketo, M. M., Birchmeier, W., and Hartmann, C. (2005) Canonical Wnt/β-catenin signaling prevents osteoblasts from differentiating into chondrocytes. *Dev Cell* **8,** 727–738
26. Rodda, S. J., and McMahon, A. P. (2006) Distinct roles for Hedgehog and canonical Wnt signaling in specification, differentiation and maintenance of osteoblast progenitors. *Development* **133,** 3231–3244
27. Joeng, K. S., Schumacher, C. A., Zylstra-Diegel, C. R., Long, F., and Williams, B. O. (2011) Lrp5 and Lrp6 redundantly control skeletal development in the mouse embryo. *Dev. Biol.* **359,** 222–229
28. Gong, Y., Slee, R. B., Fukai, N., Rawadi, G., Roman-Roman, S., Reginato, A. M., Wang, H., Cundy, T., Glorieux, F. H., Lev, D., Zacharin, M., Oexle, K., Marcelino, J., Suwairi, W., Heeger, S., *et al.* (2001) LDL receptor-related protein 5 (LRP5) affects bone accrual and eye development. *Cell* **107,** 513–523
29. Little, R. D., Carulli, J. P., Del Mastro, R. G., Dupuis, J., Osborne, M., Folz, C., Manning, S. P., Swain, P. M., Zhao, S. C., Eustace, B., Lappe, M. M., Spitzer, L., Zweier, S., Braunschweiger, K., *et al.* (2002) A mutation in the LDL receptor-related protein 5 gene results in the autosomal dominant high-bone-mass trait. *Am. J. Hum. Genet.* **70,** 11–19
30. Boyden, L. M., Mao, J., Belsky, J., Mitzner, L., Farhi, A., Mitnick, M. A., Wu, D., Insogna, K., and Lifton, R. P. (2002) High bone density due to a mutation in LDL-receptor-related protein 5. *N. Engl. J. Med.* **346,** 1513–1521
31. Balemans, W., Patel, N., Ebeling, M., Van Hul, E., Wuyts, W., Lacza, C., Dioszegi, M., Dikkers, F. G., Hildering, P., Willems, P. J., Verheij, J. B., Lindpaintner, K., Vickery, B., Foernzler, D., and Van Hul, W. (2002) Identification of a 52-kb deletion downstream of the SOST gene in patients with van Buchem disease. *J. Med. Genet.* **39,** 91–97
32. Balemans, W., Ebeling, M., Patel, N., Van Hul, E., Olson, P., Dioszegi, M., Lacza, C., Wuyts, W., Van Den Ende, J., Willems, P., Paes-Alves, A. F., Hill, S., Bueno, M., Ramos, F. J., Tacconi, P., Dikkers, F. G., Stratakis, C., Lindpaintner, K., Vickery, B., Foernzler, D., and Van Hul, W. (2001) Increased bone density in sclerosteosis is due to the deficiency of a novel secreted protein (SOST). *Hum. Mol. Genet.* **10,** 537–543
33. Kato, M., Patel, M. S., Levasseur, R., Lobov, I., Chang, B. H., Glass, D. A., 2nd, Hartmann, C., Li, L., Hwang, T. H., Brayton, C. F., Lang, R. A., Karsenty, G., and Chan, L. (2002) Cbfa1-independent decrease in osteoblast proliferation, osteopenia, and persistent embryonic eye vascularization in mice deficient in Lrp5, a Wnt coreceptor. *J. Cell Biol.* **157,** 303–314
34. Cui, Y., Niziolek, P. J., MacDonald, B. T., Zylstra, C. R., Alenina, N., Robinson, D. R., Zhong, Z., Matthes, S., Jacobsen, C. M., Conlon, R. A., Brommage, R., Liu, Q., Mseeh, F., Powell, D. R., Yang, Q. M., Zambrowicz, B., Gerrits, H., Gossen, J. A., He, X., Bader, M., Williams, B. O., Warman, M. L., and Robling, A. G. (2011) Lrp5 functions in bone to regulate bone mass. *Nat. Med.* **17,** 684–691
35. Li, X., Ominsky, M. S., Niu, Q. T., Sun, N., Daugherty, B., D'Agostin, D., Kurahara, C., Gao, Y., Cao, J., Gong, J., Asuncion, F., Barrero, M., Warmington, K., Dwyer, D., Stolina, M., Morony, S., Sarosi, I., Kostenuik, P. J., Lacey, D. L., Simonet, W. S., Ke, H. Z., and Paszty, C. (2008) Targeted deletion of the sclerostin gene in mice results in increased bone formation and bone strength. *J. Bone Miner. Res.* **23,** 860–869
36. Shechter, D., Dormann, H. L., Allis, C. D., and Hake, S. B. (2007) Extraction, purification, and analysis of histones. *Nat. Protoc.* **2,** 1445–1457
37. Esen, E., Lee, S. Y., Wice, B. M., and Long, F. (2015) PTH promotes bone anabolism by stimulating aerobic glycolysis via IGF signaling. *J. Bone Miner. Res.* **30,** 1959–1968
38. Kang, S., Bennett, C. N., Gerin, I., Rapp, L. A., Hankenson, K. D., and Macdougald, O. A. (2007) Wnt signaling stimulates osteoblastogenesis of mesenchymal precursors by suppressing CCAAT/enhancer-binding protein α and peroxisome proliferator-activated receptor gamma. *J. Biol. Chem.* **282,** 14515–14524
39. Ogawa, M., Nishikawa, S., Ikuta, K., Yamamura, F., Naito, M., and Takahashi, K. (1988) B cell ontogeny in murine embryo studied by a culture system with the monolayer of a stromal cell clone, ST2: B cell progenitor develops first in the embryonal body rather than in the yolk sac. *EMBO J.* **7,** 1337–1343
40. Eden, E., Navon, R., Steinfeld, I., Lipson, D., and Yakhini, Z. (2009) GOrilla: a tool for discovery and visualization of enriched GO terms in ranked gene lists. *BMC Bioinformatics* **10,** 48
41. Esen, E., Chen, J., Karner, C. M., Okunade, A. L., Patterson, B. W., and Long, F. (2013) WNT-LRP5 signaling induces Warburg effect through mTORC2 activation during osteoblast differentiation. *Cell Metab.* **17,** 745–755
42. Moussaieff, A., Rouleau, M., Kitsberg, D., Cohen, M., Levy, G., Barasch, D., Nemirovski, A., Shen-Orr, S., Laevsky, I., Amit, M., Bomze, D., Elena-Herrmann, B., Scherf, T., Nissim-Rafinia, M., Kempa, S., Itskovitz-Eldor, J., Meshorer, E., Aberdam, D., and Nahmias, Y. (2015) Glycolysis-mediated changes in acetyl-CoA and histone acetylation con-

trol the early differentiation of embryonic stem cells. *Cell Metab.* **21,** 392–402
43. McBrian, M. A., Behbahan, I. S., Ferrari, R., Su, T., Huang, T. W., Li, K., Hong, C. S., Christofk, H. R., Vogelauer, M., Seligson, D. B., and Kurdistani, S. K. (2013) Histone acetylation regulates intracellular pH. *Mol. Cell* **49,** 310–321
44. Meshorer, E., Yellajoshula, D., George, E., Scambler, P. J., Brown, D. T., and Misteli, T. (2006) Hyperdynamic plasticity of chromatin proteins in pluripotent embryonic stem cells. *Dev. Cell* **10,** 105–116
45. Bracha, A. L., Ramanathan, A., Huang, S., Ingber, D. E., and Schreiber, S. L. (2010) Carbon metabolism-mediated myogenic differentiation. *Nat. Chem. Biol.* **6,** 202–204